# A novel blind-deconvolution method with an application to seismology



1998 Inverse Problems 14 815

(http://iopscience.iop.org/0266-5611/14/4/004)

Inverse Problems **14** (1998) 815–833. Printed in the UK PII: S0266-5611(98)92089-5

# A novel blind-deconvolution method with an application to seismology

M Bertero†, D Bindi‡, P Boccacci§, M Cattaneo‡, C Eva‡ and V Lanza‡

† INFM and Dipartimento di Informatica, Università di Genova, Via Dodecaneso 35, I 16146 Genova, Italy

‡ Dipartimento di Scienze della Terra, Università di Genova, Viale Benedetto XV 5, I 16132 Genova, Italy

§ INFM and Dipartimento di Fisica, Università di Genova, Via Dodecaneso 33, I 16146 Genova, Italy

Received 27 February 1998

**Abstract.** The empirical Green function (EGF) model assumes that the recorded far-field waveform of an earthquake is the output of a linear system whose impulse response function is approximated by the waveform of a suitable small earthquake (the EGF) with the same focal mechanism and location as the larger one. The input of the system is the so-called source time function (STF) which describes the energy release and the rupture evolution. In a previous paper the projected Landweber method was applied to this deconvolution problem, i.e. to the estimation of the STF being given the EGF and the recorded waveform of the seismic event. The results obtained are more realistic and qualitatively much better than those provided by linear regularization methods, as a consequence of the beneficial effect of the constraints on the STF (positivity, causality, etc) introduced by means of the projected Landweber method. However, the STFs obtained in this way do not reproduce the observed seismograms within the experimental errors. This effect is presumably due to the modelling error introduced when approximating the exact (but unknown) Green function by means of the EGF so that the problem arises of improving such an approximation. To this purpose we propose a nontrivial modification of an iterative blind-deconvolution method used for image identification. The main feature of our method, which is based on the projected Landweber method, is that the use of different constraints for the EGF and STF is allowed. The convergence of the method is very fast and the results obtained in the case of synthetic and real data are quite satisfactory. Even if described and validated in the specific problem of seismology we are considering, it can be applied to any deconvolution problem where a rough approximation of the point spread function is available and different constraints must be used for the impulse response function and the input of the system.

## 1. Introduction

In a previous paper [1], hereafter referred to as I, the projected Landweber method [2] was applied to the problem of estimating the source time function (STF) of an earthquake in the framework of the empirical Green function (EGF) model. Let us recall a few basic facts about this problem.

If $G(t)$ is the Green function which describes the propagation of the seismic wave from the source point $P_0$ to the detector point $P_1$, and if $u(t)$ is the waveform recorded at $P_1$ and generated by an earthquake which occurred at $P_0$, then the STF of the earthquake is

0266-5611/98/040815+19$19.50  

defined as the function $f(t)$ such that

$$u(t) = \int_{-\infty}^{t} G(t - t') f(t') \, dt'. \tag{1}$$

Here we assume that $u(t)$ has been shifted in time to correct the time delay between the onset of the event in $P_0$ and the arrival of the wave in $P_1$. Moreover, we use the causality condition, i.e. $G(t) = 0$ for $t < 0$.

Since the computation of the Green function $G(t)$ is, in general, not very accurate, one assumes that a better approximation of $G(t)$ can be provided by the waveform of an earthquake of sufficiently small magnitude, which occurs at a point $P_0'$, close to the point $P_0$, and has the same focal mechanism as the main earthquake. This approximation of $G(t)$ is called the empirical Green function (EGF) and, in this paper, will be denoted by $G^{(0)}(t)$. The main source of error is due to the fact that the hypocentres $P_0$ and $P_0'$ of the two earthquakes do not coincide.

The measured waveform, also denoted by $u(t)$, can be written in terms of the unknown STF, $f(t)$, and of the known EGF, $G^{(0)}(t)$, as follows

$$u(t) = \int_{-\infty}^{t} G^{(0)}(t - t') f(t') \, dt' + w(t) \tag{2}$$

where $w(t)$ is an error term which describes both the noise contamination (instrumental errors, microseismic activity, etc) and the modelling error introduced by the approximate Green function $G^{(0)}(t)$. Therefore the problem of estimating the STF is a deconvolution problem in the presence of noise and errors on the impulse response function (Green function) of the system.

The projected Landweber method allows the introduction of several important constraints in this deconvolution problem:

- non-negativity: $f(t) \geqslant 0$;
- causality: $f(t) = 0$ for $t < 0$, if $u(t) = 0$ for $t < 0$;
- finite duration: $f(t) = 0$ for $t > T$.

As shown in I, this method produces estimates of the STF which are much more realistic than those provided by linear regularization methods. In particular we obtain satisfactory estimates of the Fourier transform of the STF at zero frequency. This quantity, which is important in seismology because it yields an estimate of the energy of the earthquake, cannot be obtained directly by means of linear deconvolution methods because the Fourier transform of the EGF is zero in the neighbourhood of the zero frequency (see I).

The main difficulty of the previous approach is that it provides an estimate of the STF which, in general, does not reproduce the measured waveform within the instrumental errors: the discrepancy between the computed and the real data may be of the order of 30–40% while the estimated instrumental error is of the order of 1%.

It is quite natural to argue that such a large discrepancy is mainly due to the modelling error introduced by the use of the EGF $G^{(0)}(t)$ in place of the true Green function $G(t)$. Then it is also natural to argue that this modelling error can generate large restoration errors in the estimation of the STF.

In order to improve the data fitting and to assess the reliability of the STF obtained by means of the projected Landweber method, the problem arises of obtaining an approximation of $G(t)$ which is better than that provided by $G^{(0)}(t)$. To this purpose we must use both the EGF $G^{(0)}(t)$ and the measured waveform $u(t)$.

Such a problem is very close to a *blind-deconvolution* problem, a term used in the case of image restoration and introduced by Stockham *et al* [3] for denoting a problem where

both the object and the impulse response function of the imaging system are unknown, so that both must be estimated from the knowledge of the noisy image alone. It is obvious that such a problem is affected by an extreme uncertainty about the solution so that the use of *a priori* information (constraints) is needed both about the object and about the impulse response function. To this purpose many methods have been proposed and investigated [3–6].

In the case of equation (1), the blind-deconvolution problem should consist of the estimation of both the Green function $G(t)$ and the STF $f(t)$ from the knowledge of the noisy waveform $u(t)$. However, the practical situation is more favourable if some EGF $G^{(0)}(t)$, i.e. an approximation of $G(t)$, is known. In such a case the problem could be called a quasiblind deconvolution, but we do not want to introduce a new term to indicate this particular situation.

Since $G^{(0)}(t)$ provides an approximation of $G(t)$, the most natural approach seems to be an iterative one which uses $G^{(0)}(t)$ as an initial guess and updates alternately both the Green function and the STF. More precisely the initial guess $G^{(0)}(t)$ is used for solving the deconvolution problem (1) (with $G(t) = G^{(0)}(t)$ and $f(t)$ unknown) to obtain an initial estimate $f^{(0)}(t)$ of the STF; next $f^{(0)}(t)$ is used for solving the deconvolution problem (1) (with $f(t) = f^{(0)}(t)$ and $G(t)$ as unknown) to obtain a new estimate $G^{(1)}(t)$ of the Green function and so on.

It is obvious that, if we use constrained deconvolution methods both for the Green function and STF, we must use different constraints in the two cases: the STF, for instance, is non-negative while this property does not hold true for the EGF. Since the projected Landweber method is sufficiently flexible for implementing the various kinds of constraints required by the EGF model, it is a natural candidate for solving the deconvolution problems mentioned above.

The previous remarks should make it clear that, even if the blind-deconvolution method that we propose is formulated for the specific problem of seismology we are considering, it has a wider applicability. In particular it can be applied to any imaging problem where: (1) a poor approximation of the impulse response function (point spread function) is available; (2) the impulse response function and the ideal image to be restored are subjected to different constraints. The unique restriction is that these constraints must be expressed in terms of convex sets in a Hilbert space, so that the appropriate projected Landweber method can be used.

The blind-deconvolution method is described in section 2 and validated in section 3 by means of a set of synthetic data. In section 4 we reconsider the seismograms corresponding to the events investigated in I. The main conclusion, which is discussed in detail in section 5, is that the method modifies the part of the EGF which is more affected by small perturbations in the trajectory of the seismic wave and introduces a further improvement (with respect to I) in the estimation of the STF. Moreover, the computed data are now in excellent agreement with the experimental data (the recorded seismograms).

## 2. The blind-deconvolution method

If we consider causal functions, i.e. $u(t) = G(t) = f(t) = 0$ for $t < 0$, then the basic equation (1) can be written as a standard convolution product:

$$u = G * f \tag{3}$$

and our blind-deconvolution problem can be formulated as follows: estimate $G$ and $f$, being given a noisy version of $u$ and an approximation $G^{(0)}$ of $G$. For solving this problem

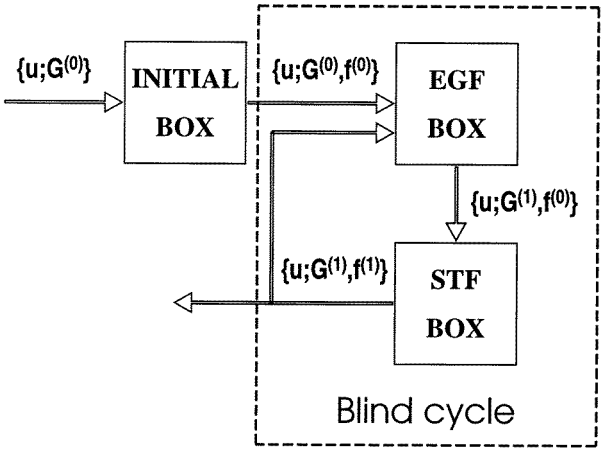


**Figure 1.** Scheme of the blind-deconvolution method. The EGF box contains the iterative method for the estimation of the EGF while the STF box contains the iterative method for the estimation of the STF.

we propose a modification of the iterative method of Ayres and Dainty [4] which is based on the symmetry of the convolution product and consists of using the same deconvolution method for estimating alternately $G$ and $f$. Since, as already observed in the introduction, $G$ and $f$ have different properties, the use of the same deconvolution method for $G$ and $f$ is not the most convenient approach to our problem.

In order to simplify our presentation we give a pictorial representation of the method in figure 1 and we refer to this figure when describing the various steps of the procedure.

The data of the problem are the measured waveform $u(t)$ and the measured EGF $G^{(0)}(t)$. With these data we can estimate an approximate solution of the convolution equation $u = G^{(0)} * f$, having the correct properties indicated in the introduction: non-negativity, causality and finite duration. To this purpose we can use the method described in I and based on the projected Landweber method. The estimate of the unknown duration $T$ of the STF can be obtained, as shown in I, by looking at the behaviour of the residual as a function of $T$.

This procedure provides an estimate $f^{(0)}(t)$ of $f(t)$, which is non-negative and zero outside a certain interval $(0, T)$. This procedure is the content of the initial box indicated in figure 1: the input is the pair of measured functions $\{u(t), G^{(0)}(t)\}$, the output is the triple $\{u(t); G^{(0)}(t), f^{(0)}(t)\}$ such that $u \simeq G^{(0)} * f^{(0)}$. As already remarked in the introduction, however, $G^{(0)}$ and $f^{(0)}$ do not reproduce the measured waveform $u$ within the experimental errors, i.e. the relative residual

$$\varepsilon^{(0)} = \frac{\|G^{(0)} * f^{(0)} - u\|_2}{\|u\|_2} \tag{4}$$

is too large. Here we use the notation

$$\|h\|_2 = \int_0^{+\infty} |h(t)|^2 \, \mathrm{d}t \tag{5}$$

if $h(t)$ is a causal and square-integrable function.

The triple $\{u; G^{(0)}, f^{(0)}\}$ is the input of the EGF box, as indicated in figure 1. Here we consider as data the waveform $u(t)$ and the estimate $f^{(0)}(t)$ of the STF and we look for a new estimate $G^{(1)}(t)$ of the EGF by solving the convolution equation $u = f^{(0)} * G$. The

deconvolution method is the projected Landweber method with the constraint of causality. As an initial guess of this iterative deconvolution method we use the EGF $G^{(0)}(t)$. The precise algorithm will be described shortly. The box must also contain a criterion for stopping the iterations. The result of the last iteration is the new estimate $G^{(1)}(t)$ of the Green function.

The output $\{u; G^{(1)}, f^{(0)}\}$ of the EGF box is the input of the subsequent STF box. Here we consider as data the waveform $u(t)$ and the new estimate $G^{(1)}(t)$ of the EGF and we look for a new estimate $f^{(1)}(t)$ of the STF by solving the convolution equation $u = G^{(1)} * f$. The deconvolution method used is the projected Landweber method with the constraints of positivity and of boundedness of the support. The support of the STF is the interval $(0, T)$ obtained in the initial box. Moreover, the initial guess of the iterations is the previous estimate $f^{(0)}(t)$ of the STF. Again the precise algorithm will be described shortly. The box must also contain a criterion for stopping the iterations. The result of the last iteration is the new estimate $f^{(1)}(t)$ of the STF.

The output $\{u; G^{(1)}, f^{(1)}\}$ of the STF box is also the output of the first blind cycle, i.e. a cycle consisting of one EGF and one STF box. The relative residual $\varepsilon^{(1)}$, associated with this triple, can be computed. If it is of the order of the relative rms error affecting the data, we can stop the procedure, otherwise the triple $\{u; G^{(1)}, f^{(1)}\}$ is used for initializing a second blind cycle and so on. Therefore the algorithm consists of a sequence of blind cycles and, inside each blind cycle, of two iterative constrained Landweber methods, one for estimating the EGF and one for estimating the STF.

We now give a more precise description of the algorithm and to this purpose we introduce the following notations.

• For any square-integrable function $h(t)$, we denote by $h_-(t)$ the reflected function defined by

$$h_-(t) = h(-t). \tag{6}$$

• We denote by $\mathcal{P}_\mathcal{C}$ the projection operator onto the linear subspace of the causal functions, i.e.

$$(\mathcal{P}_\mathcal{C} h)(t) = \begin{cases} h(t) & \text{if } t > 0 \\ 0 & \text{if } t < 0. \end{cases} \tag{7}$$

• We denote by $\mathcal{P}_\mathcal{S}$ the projection operator onto the closed and convex set (in $L^2(\mathbb{R})$) of the non-negative functions with support in the closed interval $[0, T]$, i.e

$$(\mathcal{P}_\mathcal{S} h)(t) = \begin{cases} h(t) & \text{if } h(t) > 0 \text{ and } t \in [0, T] \\ 0 & \text{elsewhere.} \end{cases} \tag{8}$$

Let $\{u; G^{(k-1)}, f^{(k-1)}\}$ be the output of the $(k-1)$th cycle; then the two boxes of the $k$th cycle contain the following algorithms.

### *2.1. EGF box*

The basic equation is

$$u = f^{(k-1)} * G. \tag{9}$$

The updating of the EGF is obtained by applying to this equation the projected Landweber method with the causality constraint, using $G^{(k-1)}$ as an initial guess. If we denote by $G_m^{(k)}$

($m = 0, 1, 2, \ldots$), the result of the $m$th iteration, the iterative scheme is as follows

$$\begin{aligned} G_0^{(k)} &= G^{(k-1)} \\ G_{m+1}^{(k)} &= \mathcal{P}_{\mathcal{C}}\{G_m^{(k)} + \sigma^{(k)} f_-^{(k-1)} * (u - f^{(k-1)} * G_m^{(k)})\} \end{aligned} \tag{10}$$

where $\sigma^{(k)}$ is the relaxation parameter, satisfying the conditions

$$0 < \sigma^{(k)} < \frac{2}{\|\hat{f}^{(k-1)}\|_\infty^2}. \tag{11}$$

Here $\hat{f}^{(k-1)}$ is the Fourier transform of $f^{(k-1)}$ and

$$\|\hat{f}^{(k-1)}\|_\infty = \sup_\omega |\hat{f}^{(k-1)}(\omega)|. \tag{12}$$

The box must also contain a criterion for stopping the iterations. In the case of synthetic data, if $G(t)$ is the Green function used for generating the synthetic waveform $u(t)$, at each iteration step we compute the relative restoration error

$$\gamma_m^{(k)} = \frac{\|G_m^{(k)} - G\|_2}{\|G\|_2} \tag{13}$$

and the stopping rule consists of stopping the iterations when we find the minimum of $\gamma_m^{(k)}$.

In any case, the stopping rule used implies that only a certain number $M$ of iterations is performed ($M$ depends, in general, on the order $k$ of the blind cycle) and the result of the $M$th iteration is the update of $G^{(k-1)}$, i.e.

$$G^{(k)} = G_M^{(k)}. \tag{14}$$

*Remark.* The iterative method of the EGF box is written as a projected Landweber method because this is the form convenient for the implementation in terms of the Fourier transform (see I). However, thanks to the linearity of the projection operator $\mathcal{P}_{\mathcal{C}}$, the algorithm (10) is equivalent to a standard Landweber method. If we introduce the following operator (which is an integral operator of the Wiener–Hopf class)

$$F^{(k-1)}h = \mathcal{P}_{\mathcal{C}}(f_-^{(k-1)} * f^{(k-1)}) * h \tag{15}$$

and if we consider the following iterative scheme

$$\begin{aligned} G_0^{(k)} &= G^{(k-1)} \\ G_{m+1}^{(k)} &= \sigma^{(k)}\mathcal{P}_{\mathcal{C}} f_-^{(k-1)} * u + (I - \sigma^{(k)} F^{(k-1)}) G_m^{(k)} \end{aligned} \tag{16}$$

then it is easy to prove, by induction, that $\mathcal{P}_{\mathcal{C}} G_{m+1}^{(k)} = G_{m+1}^{(k)}$. It follows that the $G_{m+1}^{(k)}$ given by equation (10) coincides with the $G_{m+1}^{(k)}$ given by equation (16). Since the algorithm (10) is a standard Landweber method, the existence of the minimum of $\gamma_m^{(k)}$, as a function of $m$, is assured by the semiconvergence property of this method [2].

### *2.2. STF box*

The basic equation is

$$u = G^{(k)} * f. \tag{17}$$

The updating of the STF is obtained by applying to this equation the projected Landweber method with the constraints of positivity and of boundedness of the support (interval $[0, T]$),

using $f^{(k-1)}$ as initial guess. If we denote by $f_n^{(k)}$ ($n = 0, 1, 2, \ldots$), the result of the $n$th iteration, the iterative scheme is as follows

$$\begin{aligned} f_0^{(k)} &= f^{(k-1)} \\ f_{n+1}^{(k)} &= \mathcal{P}_{\mathcal{S}}\{f_n^{(k)} + \tau^{(k)} G_-^{(k)} * (u - G^{(k)} * f_n^{(k)})\} \end{aligned} \tag{18}$$

where $\tau^{(k)}$ is the relaxation parameter, satisfying the conditions

$$0 < \tau^{(k)} < \frac{2}{\|\hat{G}^{(k)}\|_\infty^2} \tag{19}$$

and

$$\|\hat{G}^{(k)}\|_\infty = \sup_\omega |\hat{G}^{(k)}(\omega)|. \tag{20}$$

Also this box must contain a stopping rule. In the case of synthetic data, if $f(t)$ is the STF used for generating $u(t)$, at each iteration step we compute the relative restoration error

$$\delta_n^{(k)} = \frac{\|f_n^{(k)} - f\|_2}{\|f\|_2}. \tag{21}$$

Then the stopping rule consists of stopping the iterations when we find the minimum of $\delta_n^{(k)}$ or when we find that this quantity does not change in a significant way. In such a case, indeed, the semiconvergence property is not proved.

In any case, the stopping rule used implies that only a certain number $N$ of iterations is performed (also $N$ depends, in general, on the order $k$ of the blind cycle) and the result of the $N$th iteration is precisely the update of $f^{(k)}$, i.e.

$$f^{(k)} = f_N^{(k)}. \tag{22}$$

In conclusion, at the exit of the $k$th blind cycle we have the triple $\{u; G^{(k)}; f^{(k)}\}$, $G^{(k)}$ and $f^{(k)}$ being given respectively by equations (14) and (22). Then we compute the relative residual

$$\varepsilon^{(k)} = \frac{\|G^{(k)} * f^{(k)} - u\|_2}{\|u\|_2} \tag{23}$$

and we can possibly stop the blind cycles if this quantity is of the order of the experimental errors (discrepancy criterion).

We conclude this section with a few comments about the convergence of the method.

As is well known, the semiconvergence of the Landweber or of the projected Landweber method is, in general, rather slow, in the sense that a large number of iterations may be required for reaching the minimum of the restoration error. If we denote by $n_{\text{opt}}$ this number, then, for a given problem, $n_{\text{opt}}$ depends both on the amount of the noise corrupting the data and on the value of the relaxation parameter, i.e. the parameter $\sigma^{(k)}$ of equation (10) or the parameter $\tau^{(k)}$ of equation (18).

In view of the noise dependence, $n_{\text{opt}}$ increases when the amount of noise decreases (see, for instance, [2, ch 6]). Since in the problem considered in this paper the noise is small we should expect a large number of iterations. This is not true, at least in the first blind cycles, and we think that this behaviour is due to the large modelling error. In other words the semiconvergence of the method is fast in the presence of large noise and/or modelling errors.

In view of the dependence of $n_{\text{opt}}$ on the relaxation parameter, let us write the parameters of equations (10) and (18) in the following form

$$\sigma^{(k)} = \frac{\alpha^{(k)}}{\|\hat{f}^{(k-1)}\|_\infty^2} \qquad \tau^{(k)} = \frac{\beta^{(k)}}{\|\hat{G}^{(k)}\|_\infty^2} \tag{24}$$

with $0 < \alpha^{(k)}, \beta^{(k)} < 2$. When $\alpha^{(k)}$ (or $\beta^{(k)}$) increases, $n_{\text{opt}}$ first decreases, reaches a minimum and then increases again, for values of $\alpha^{(k)}$ (or $\beta^{(k)}$) close to 2 (see again [2, ch 6]). Since the determination of the optimal choice may be difficult and since its value is not very crucial in our problem, for the reasons explained above, we have used equation (24) with $\alpha^{(k)} = \beta^{(k)} = 1$.

## 3. Validation of the method by means of synthetic data

In order to validate the method described in the previous section, we use three sets of EGF corresponding to three different seismic events. Each set consists of the waveforms registered at three stations of the IGG network (see I), denoted by ROB, IMI and PCP. These waveforms are obtained by interpolating, resampling and filtering the raw data. The procedure is briefly described in I.

The first two sets of EGF, denoted by EGF42 and EGF48 and already used in I, correspond to events which occurred during a seismic swarm in July 1993. The second set of EGF, denoted by EGFDec, corresponds to an event which occurred five months later in December 1993, during a reactivation of the same seismogenetic zone. However, as pointed out in [7], the earthquakes of this second swarm have a slightly different location with respect to those of July 1993, which are considerably shallower than the events which occurred in December. Hence, if we generate synthetic waveforms by means of the EGF of the set EGF42, the EGF of the sets EGF48 and EGFDec provide approximations, with different degrees of accuracy, of the true EGF and can be used for validating the blind-deconvolution method.

The EGF of the three sets are shown in figure 2. The length of these records is about 200 samples with a sampling distance of 5 ms. In order to take into account causality, the records have been extended to a length of 512 samples by zero padding. The three sets

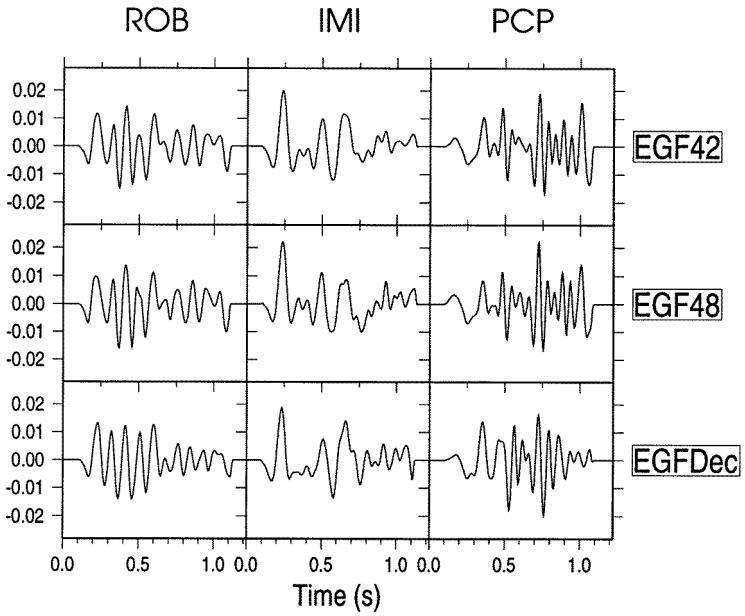


**Figure 2.** The three sets of EGF used for the validation of the blind-deconvolution method.

**Table 1.** The values of $\gamma^{(0)}$ for the three stations considered in this paper.

| $\gamma^{(0)}$ | ROB | IMI | PCP |
|---|---|---|---|
| EGF48 | 0.20 | 0.32 | 0.40 |
| EGFDec | 0.56 | 0.48 | 0.98 |

of EGF have also been normalized in such a way that the sum of the modulus of their samples is 1. Moreover, for each station, the alignment of the corresponding triple of EGF has been defined both by maximizing the cross-correlation function and by minimizing the Euclidean norm of their difference. The alignments obtained by the two methods coincide. The relative similarity of an element of EGF48 or EGFDec (denoted by $G$) with respect to the corresponding element of EGF42 (denoted by $G_{42}$) can be measured by the quantity

$$\gamma^{(0)} = \frac{\|G - G_{42}\|_2}{\|G_{42}\|_2} \tag{25}$$

where the norm is now the Euclidean one. The values of $\gamma^{(0)}$ are reported in table 1.

As we see, for EGF48 the average difference is about 30% while for EGFDec it is about 50% in the case of ROB and IMI stations and about 100% in the case of the PCP station. In this way we confirm that we have a set of EGF which reproduce, with various degrees of approximation, those used for generating the synthetic data.

In addition, we consider three models of STF with Gaussian shapes. If we give the variance $\sigma$ of a Gaussian in terms of the number of samples and its height $a$ in arbitrary units, then the three models are the following:

(1) Gaussian with $\sigma = 2$ and $a = 1800$;
(2) Gaussian with $\sigma = 5$ and $a = 720$;
(3) superposition of two Gaussians, the former with $\sigma_1 = 2$, $a_1 = 1000$ and the latter with $\sigma_2 = 4$, $a_2 = 400$, the distance between the two maxima being $d = 13$.

For each station, these EGF are convolved with the corresponding EGF42 and in such a way causal waveforms are obtained. Finally, the nonzero section of the signal is perturbed, as in I, by adding the noise obtained from a window of about 1 second on the trace of the EGF (also resampled and filtered) a few seconds before the P-wave arrival. In conclusion a set of nine waveforms, three for each model, is generated by means of EGF42, with a noise-to-signal ratio of the order of 0.5%.

In order to apply the algorithm described in section 2, the first step is to deconvolve the synthetic data by means of the method proposed in I. This is the content of the so-called initial box. Of course data can be deconvolved using EGF42 as well as EGF48 and EGFDec. In order to measure the quality of the restoration we compute the relative restoration error

$$\delta^{(0)} = \frac{\|f^{(0)} - f\|_2}{\|f\|_2} \tag{26}$$

where $f^{(0)}$ is the estimation of the model function $f$, obtained in the initial box, and the norm is again the Euclidean one. At the output of the initial box we also compute the quantity $\varepsilon^{(0)}$ which is defined as in equation (4), with the Euclidean norm now replacing the $L^2$-norm.

The results obtained in the initial box are reported in figure 3. As we see, if we deconvolve the data by means of the same EGF used for generating the data, the values

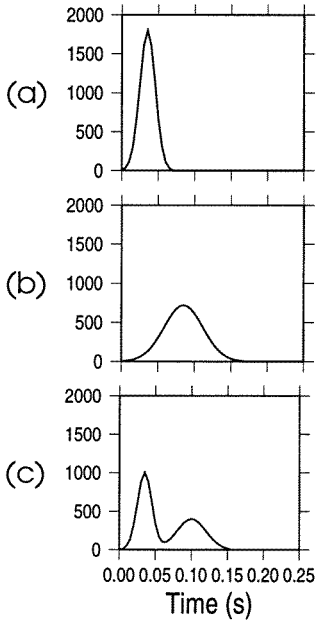


| | EGF42 | | EGF48 | | EGFDec | |
|---|---|---|---|---|---|---|
| | $\delta^{(0)}$ | $\varepsilon^{(0)}$ | $\delta^{(0)}$ | $\varepsilon^{(0)}$ | $\delta^{(0)}$ | $\varepsilon^{(0)}$ |
| ROB | 0.13 | 0.007 | 0.21 | 0.18 | 0.28 | 0.50 |
| IMI | 0.18 | 0.018 | 0.24 | 0.27 | 0.44 | 0.40 |
| PCP | 0.07 | 0.003 | 0.23 | 0.25 | 0.44 | 0.80 |
| ROB | 0.01 | 0.003 | 0.09 | 0.21 | 0.09 | 0.48 |
| IMI | 0.03 | 0.004 | 0.12 | 0.32 | 0.11 | 0.33 |
| PCP | 0.01 | 0.002 | 0.10 | 0.36 | 0.33 | 0.80 |
| ROB | 0.16 | 0.018 | 0.24 | 0.19 | 0.38 | 0.51 |
| IMI | 0.19 | 0.018 | 0.33 | 0.49 | 0.44 | 0.38 |
| PCP | 0.07 | 0.005 | 0.20 | 0.32 | 0.55 | 0.78 |

**Figure 3.** Results obtained in the initial box of the blind-deconvolution method. The shape of each STF is given together with the table reporting the results provided by the three sets of EGF, using the projected Landweber method.

of $\varepsilon^{(0)}$ are of the order of the noise affecting the data, while if we deconvolve the data by means of a different EGF the discrepancy is very large: of the order of 20% in the case of EGF48 and of the order of 50% in the case of EGFDec. As expected the discrepancy increases when the modelling error increases.

The situation is more complex when considering the restoration error $\delta^{(0)}$. In the case of the broad Gaussian the restoration error, when using EGF42, is of the order of the error affecting the data, while it is much larger (except in the case of the PCP station) for model (a) and model (c). The reason is that, in such a case, the band of the narrow Gaussian is broader than the band of the EGF and therefore, as discussed in I, the restoration of the STF requires out-of-band extrapolation.

This remark does not apply to the EGF of the PCP station, whose band is considerably broader than that of the EGF of ROB and IMI. In other words, in the case of PCP the low-pass filtering due to propagation is not so strong as in the case of the other stations. This interpretation is confirmed by the Fourier spectra of EGF48 and EGFDec for PCP: in both cases the band is comparable with that of EGF42 even if the spectra are considerably different.

In conclusion, since the band of EGF42 for the PCP station is comparable with the band of the narrow Gaussian, the restoration is quite good also in the case of the models (a) and (c).

A general remark on the restoration errors $\delta^{(0)}$ obtained by means of EGF48 and EGFDec is that, as shown in figure 3, these errors are smaller in the case of EGF48 than in the case of EGFDec (except for two stations in the case of model (b)) and, in general, are much greater than those obtained by means of the correct EGF. Therefore we find confirmation of the fact that also the restoration error increases when the modelling error increases.

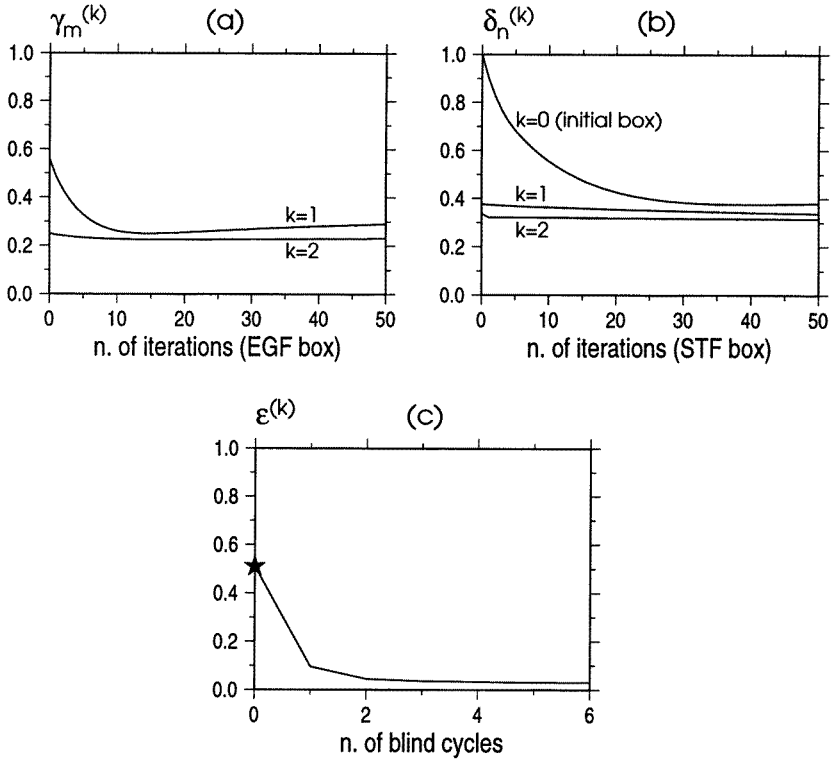


**Figure 4.** (*a*) Behaviour of the restoration error $\gamma_m^{(k)}$, equation (13), as a function of the number $m$ of iterations in the EGF box for the first two blind cycles ($k = 1, 2$); (*b*) behaviour of the restoration error $\delta_n^{(k)}$, equation (21), as a function of the number $n$ of iterations in the initial box ($k = 0$) compared with the behaviour of the restoration error in the STF box for the first two blind cycles ($k = 1, 2$); (*c*) behaviour of the relative residual $\varepsilon^{(k)}$, equation (23), as a function of the number of blind cycles. The case considered is that of the STF (*c*) of figure 3, station ROB, EGFDec.

In view of the blind-deconvolution method described in the previous section, we have first applied the method to the case of EGF42, i.e. we have used the correct EGF as an initial guess. We have verified that, after several blind cycles, neither the EGF nor the STF estimated in the initial box are modified in a significant way. Therefore we can conclude that, in a practical case, if we have at our disposal the correct EGF, this is not corrupted by the blind method.

The behaviour of the method in the case of EGF48 and EGFDec is quite interesting. At the first blind cycle the restoration error in the EGF box has a minimum which occurs after a few Landweber iterations (of the order of 5 in the case of a short event and of the order of 10 in the case of a broader one), as shown in figure 4(*a*). On the other hand, the restoration error in the STF box is practically constant after one or two Landweber iterations and smaller than the minimum restoration error obtained in the initial box, as shown in figure 4(*b*).

At the second blind cycle the restoration error is constant after one or two iterations both in the EGF and STF box—see again figures 4(*a*) and (*b*)—and a bit smaller than that obtained in the first blind cycle. The flat behaviour of the restoration errors is observed also in the subsequent blind cycles and, in general, after the third cycle they do not change in a

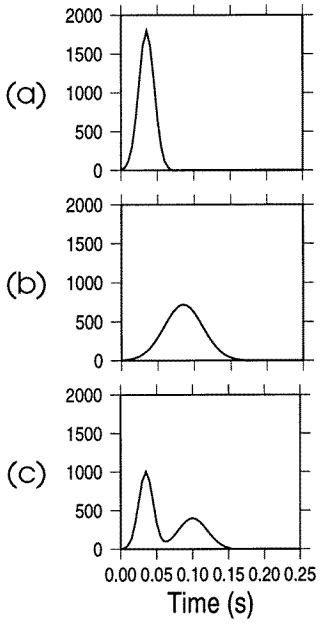


| | EGF48 | | | | EGFDec | | | |
|---|---|---|---|---|---|---|---|---|
| | $\delta^{(0)}$ | $\delta$ | $\gamma$ | $\varepsilon$ | $\delta^{(0)}$ | $\delta$ | $\gamma$ | $\varepsilon$ |
| ROB | 0.21 | 0.19 | 0.10 | 0.002 | 0.28 | 0.21 | 0.19 | 0.006 |
| IMI | 0.24 | 0.23 | 0.10 | 0.003 | 0.44 | 0.39 | 0.21 | 0.002 |
| PCP | 0.23 | 0.22 | 0.29 | 0.002 | 0.44 | 0.33 | 0.54 | 0.006 |
| ROB | 0.09 | 0.06 | 0.12 | 0.004 | 0.09 | 0.08 | 0.33 | 0.020 |
| IMI | 0.12 | 0.09 | 0.13 | 0.003 | 0.11 | 0.09 | 0.18 | 0.006 |
| PCP | 0.10 | 0.08 | 0.37 | 0.008 | 0.33 | 0.32 | 0.78 | 0.021 |
| ROB | 0.24 | 0.21 | 0.11 | 0.005 | 0.38 | 0.28 | 0.21 | 0.024 |
| IMI | 0.33 | 0.24 | 0.19 | 0.010 | 0.44 | 0.35 | 0.27 | 0.010 |
| PCP | 0.20 | 0.17 | 0.33 | 0.010 | 0.55 | 0.40 | 0.50 | 0.020 |

**Figure 5.** Summary of the results obtained by means of the blind-deconvolution method in the case of synthetic data. We recall that $\gamma$ is the relative error in the estimation of EGF42 by means of EGF48 and EGFDec, respectively, at the end of the blind iterations; $\delta$ is the relative restoration error in the estimation of the STF at the end of the blind iterations and $\varepsilon$ is the corresponding residual.

significant way. In conclusion, the procedure is convergent after a small number of blind cycles (let us say, three) and the result remains stable during the subsequent cycles. In view of the behaviour of $\varepsilon^{(k)}$, equation (23), it decreases rapidly after the first blind cycles and becomes of the order of the experimental errors, as shown in figure 4($c$).

The results obtained by applying the method to the various models of STF given in figure 3, both in the case of EGF48 and in the case of EGFDec, are reported in figure 5. Here $\delta$ denotes the relative error in the restoration of the STF, defined as in equation (21), with $f_n^{(k)}$ corresponding to the last Landweber iteration in the last blind cycle. Analogously $\gamma$ denotes the relative error in the estimation of EGF42, defined as in equation (13) with $G_n^{(k)}$ corresponding to the last Landweber iteration in the last blind cycle. In all cases we used three blind cycles.

Let us give a few comments about these results. The reported values of $\delta$ are always smaller than the values of $\delta^{(0)}$; in some cases the improvement is significant while in others it is rather small. The largest improvements are obtained in the case of EGFDec, the worse approximation of EGF42. This result implies that the blind method is important, especially when the approximation provided by the EGF is very rough. In any case the values of $\delta$ obtained by means of EGFDec are greater than those obtained by means of EGF48 and both are greater than the values of $\delta^{(0)}$ obtained by means of the correct EGF, i.e. EGF42, and reported in figure 3.

In view of the values of $\gamma$ reported in figure 5, they are considerably smaller than the corresponding values of $\gamma^{(0)}$ given in table 1. Moreover, the improvement does not strongly depend, in general, on the STF used in the blind method. In the case of the short event ($a$) and of ROB and IMI stations, the approximations obtained are quite good but are

satisfactory also when a longer event is used. This remark does not apply to the case of EGFDec and PCP station but in such a case the difference between EGF42 and EGFDec is too large.

We have also applied the method to the case of data generated by means of a very broad Gaussian ($\sigma = 10$). The difficulty in such a case is that the band of the STF and therefore also the band of the waveform is narrower than the band of the EGF. In other words the data do not contain information about the Fourier transform of the EGF on a significant part of its band. This remark explains the failure of the blind method in this case. After a reasonable number of blind cycles, 10–20, the restoration of the STF is not modified with respect to the initial box, while the EGF is modified in an unacceptable way. Indeed the EGF obtained when the results of the iterations are stable is very different from the initial one and has a band which approximately coincides with the band of the data.

In conclusion, while the restoration of the STF is not very sensitive to the EGF used and can be a bit improved by means of the blind method, this method provides a considerable improvement of the EGF. Moreover the estimated STF and EGF reproduce the waveforms within the experimental errors, as follows from the values of $\varepsilon$ reported in figure 5. A few examples of the results we have obtained are given in figure 6.

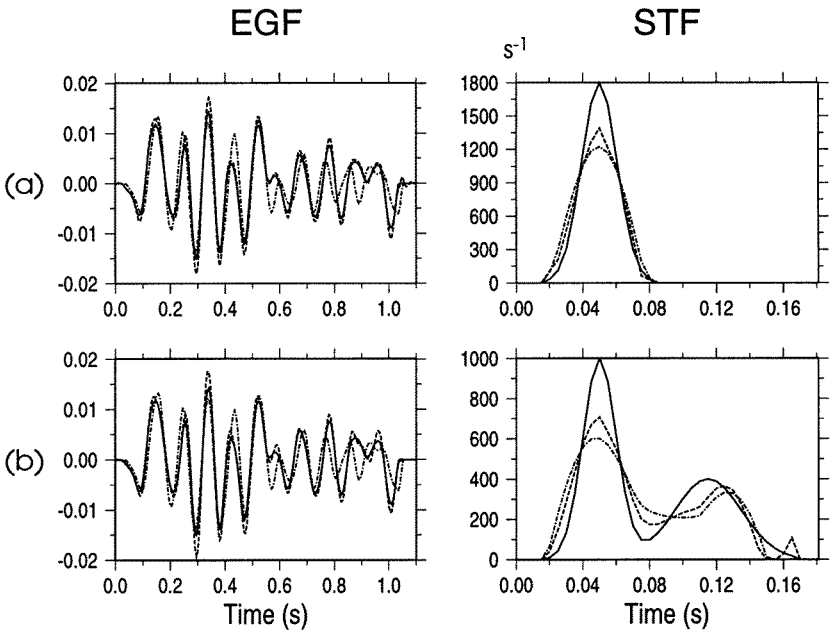


**Figure 6.** Examples of results obtained by means of the blind method. Full curves correspond to EGF42 and to the STF used for generating the synthetic data; chain curves correspond to EGFDec and to the restored STF obtained in the initial box; broken curves correspond to the EGF and STF obtained by applying the blind method. The station is ROB. In the case of the narrow Gaussian, the difference between EGF42 and EGF obtained by applying the blind method to EGFDec is not visible. The improvement in the restoration of the STF as provided by the blind method is significant in both cases.

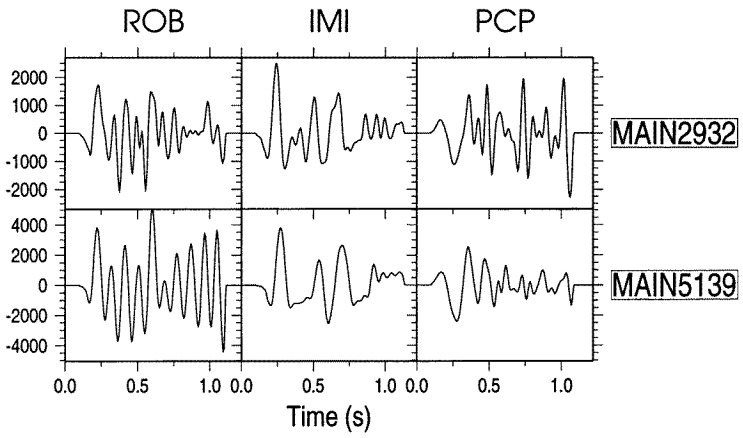


**Figure 7.** The waveforms of the main events.

## 4. Application of the method to real data

The results described in the previous section suggest the following methods for the application of the blind method to real data (here denoted as the main waveform).

(i) Compute the Fourier transform of the EGF and of the main waveform and estimate their bands. If the bandwidth of the main is smaller than or approximately equal to that of the EGF, then the blind method can be used, while it is certainly useless if the bandwidth of the main waveform is considerably smaller than that of the EGF.

(ii) By means of the method implemented in the initial box, estimate the support $(0, T)$ of the STF which generates the main waveform. If this interval is much shorter than the length of the record, then the main event can be classified as a simple one, otherwise it is classified as a complex event.

(iii) In the EGF box of the first blind cycle use about five iterations in the case of a simple event and 10 in the case of a complex one. In both cases use about 10 iterations in the STF box (such a large number of iterations may be unnecessary, but the algorithm is very fast, since it is Fourier based, as described in I).

(iv) In the subsequent blind cycles use 10 iterations both in the EGF and in the STF box (also in this case the number of iterations is overestimated).

(v) Stop the procedure when the relative residual at the exit of the last blind cycle is of the order of the relative rms error on the data (in this application, about 1%).

We have applied the method to the main waveforms of the events already considered in I. They are shown in figure 7 for the three stations ROB, IMI and PCP, corresponding to the EGF used in section 3. The blind method must be applied for all these EGF which provide approximations (with a different, but unknown, degree of accuracy) of the correct Green functions of the main events. We expect that EGF42 and EGF48 are better approximations than EGFDec, because their hypocentres are closer to those of the main events than the hypocentre of EGFDec. In addition, the results obtained in I indicate EGF42 as the candidate to provide the best approximation of the unknown Green function.

In the initial box we adopt a procedure which does not correspond exactly to that used in I. We first do a rough choice of the support of the STF and we use the projected Landweber method corresponding to this choice and to the positivity constraint. In order to stop the Landweber iterations, the well known discrepancy principle [8] cannot be used because the

**Table 2.** Values of $\varepsilon^{(0)}$ at the output of the initial box.

| | MAIN2932 | | | MAIN5139 | | |
|---|---|---|---|---|---|---|
| | EGF42 | EGF48 | EGFDec | EGF42 | EGF48 | EGFDec |
| ROB | 0.51 | 0.52 | 0.64 | 0.59 | 0.55 | 0.66 |
| IMI | 0.30 | 0.32 | 0.53 | 0.25 | 0.39 | 0.32 |
| PCP | 0.35 | 0.46 | 0.32 | 0.63 | 0.69 | 0.43 |

residual is always much greater than the estimated rms error on the data. On the other hand the generalized discrepancy principle [8] cannot be used because the error on the EGF is not known. Therefore we use the following observation.

If we denote by $f_n^{(0)}$ the result of the $n$th Landweber iteration in the initial box, its relative discrepancy, defined by

$$\varepsilon_n^{(0)} = \frac{\|G^{(0)} * f_n^{(0)} - u\|_2}{\|u\|_2} \tag{27}$$

has a typical behaviour as a function of $n$: first it rapidly decreases and then becomes essentially flat, with a change of slope which occurs at a rather well defined value of $n$. As a consequence of this behaviour we decide to stop the iterations at the value of $n$, let us say $n_0$, corresponding to the beginning of the flat behaviour of $\varepsilon_n^{(0)}$. This value depends on the quality of the $G^{(0)}$ used: the worse $G^{(0)}$, the higher the number of iterations required for reaching the stability of $\varepsilon_n^{(0)}$.

Once $n_0$ is determined, with this number of iterations we compute the residual corresponding to different choices of the support of the STF and its behaviour is used for estimating a more appropriate support of the STF (see I). The values of $\varepsilon^{(0)}$ obtained in such a way at the exit of the initial box are reported in table 2. We observe that in the case of MAIN2932 the values of $\varepsilon^{(0)}$ provided by EGF42 and EGF48 are smaller than those provided by EGFDec for ROB and IMI stations and greater for PCP station. In the case of MAIN5139 the situation is even more complex.

The blind method is applied to the output of the initial box, using the rules indicated at the beginning of this section. The results are shown in figure 8 where the STF obtained at the end of the blind method are compared with the outputs $f^{(0)}$ of the initial box. The different normalizations of the STF of the same event obtained with different EGF are due to the different magnitudes of the events providing the EGF.

The first important remark is the considerable qualitative agreement between the STF of the same event obtained by means of the various EGF even where the outputs of the initial box are considerably different. This fact is very evident in the case of MAIN2932 and ROB station and also in the case of MAIN5139 and ROB and PCP stations. In all cases the agreement is satisfactory in view of the shape and duration of the event. These results are also consistent with those obtained in I (without the blind method) using EGF42.

In conclusion, if the approximation of the EGF is not too poor, the projected Landweber method (without blind deconvolution) can provide a reliable estimate of the STF even if this is unable to reproduce the recorded waveform. Similar results can be obtained, using the blind method, even when the approximation of the EGF is much poorer.

The beneficial effect of the blind deconvolution is even more evident if we look at the spectrum of the STF. This effect is illustrated in figure 9 in the case of MAIN2932 and ROB station, where we compare the spectra obtained by means of EGF42 and EGFDec (upper panels) before and after blind deconvolution. In the case of EGF42 the two spectra

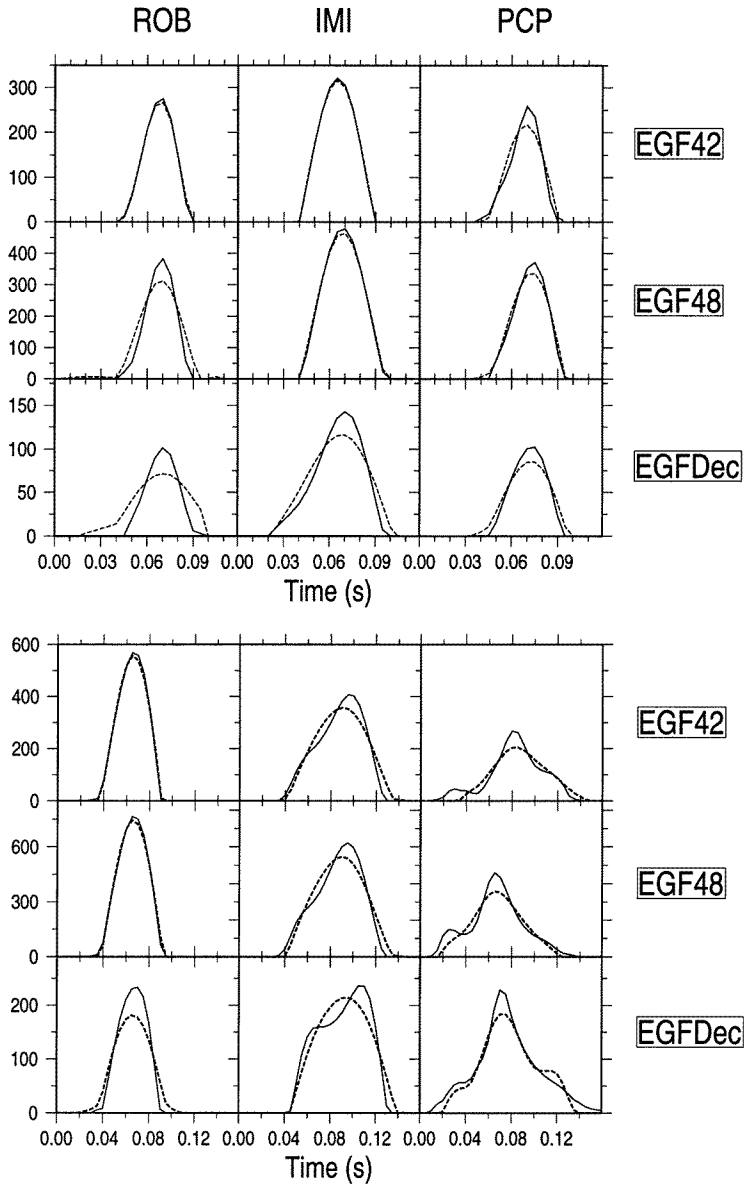


**Figure 8.** Comparison of the estimates $f^{(0)}$ obtained in the initial box (broken curves) with the STF obtained by means of the blind method (full curves) in the case of MAIN2932 (top panels) and in the case of MAIN5139 (bottom panels).

essentially coincide while they are quite different in the case of EGFDec. After blind deconvolution the spectrum obtained by means of EGFDec is in good agreement with that obtained by means of EGF42.

In the same figure we give also the spectra of the EGF before and after the blind method. It is evident that the spectra of EGF42 and EGFDec after blind deconvolution are much more similar than before. Another interesting effect in this example is the broadening of

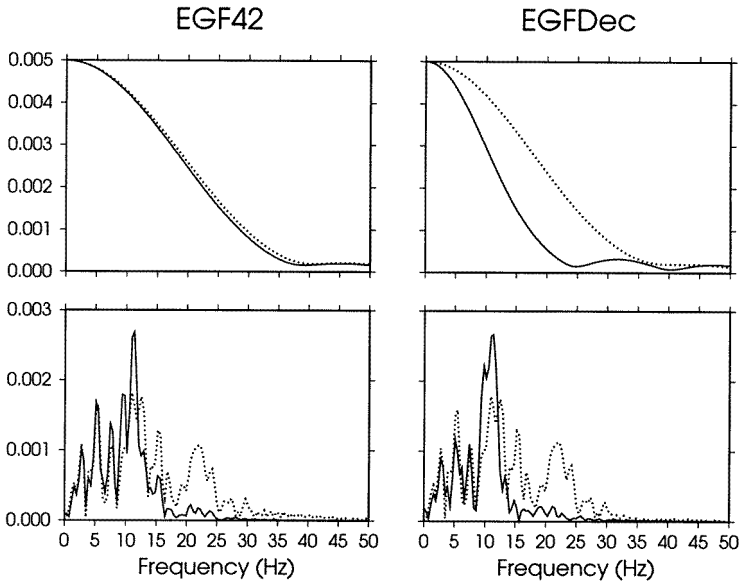


**Figure 9.** Upper panels: comparison of the spectra (modulus of the Fourier transform) obtained by means of EGF42 and EGFDec in the case of MAIN2932, ROB station. Full curves refer to the outputs of the initial box and dotted curves refer to the outputs of the blind method. Lower panels: comparison of the spectra of the EGF before blind method (full curves) and after blind method (dotted curves).

**Table 3.** Values of the peaks of the cross-correlation function of all pairs of EGF before and after the blind method. Main 5139.

| | $C_{42-48}$ | | $C_{42-Dec}$ | | $C_{48-Dec}$ | |
|---|---|---|---|---|---|---|
| | Before | After | Before | After | Before | After |
| ROB | 0.97 | 0.99 | 0.84 | 0.98 | 0.81 | 0.99 |
| IMI | 0.95 | 0.99 | 0.88 | 0.95 | 0.80 | 0.95 |
| PCP | 0.95 | 0.90 | 0.51 | 0.93 | 0.55 | 0.95 |

the band of the EGF provided by the blind method.

As a general comment we can state that the blind method increases the similarity of different EGF. This effect may be considered obvious in the case of MAIN2932 because this is a simple event. However, it holds true also in the case of MAIN5139. This effect is quantified in table 3 where we report the values of the peaks of the cross-correlation functions of all pairs of EGF before and after the blind method.

As already observed, the blind method produces a considerable modification of the EGF. However this modification is reasonable from the physical point of view because, in general, it concerns mainly the second part of the EGF, namely that part which is more sensitive to small perturbations in the trajectory of the seismic wave and therefore it is more sensitive to the location of the event. This effect is shown in figure 10.

Finally, also in the case of real data, we find that the STF and EGF obtained by means of the blind method reproduce the recorded main waveforms in excellent agreement with the experimental data.

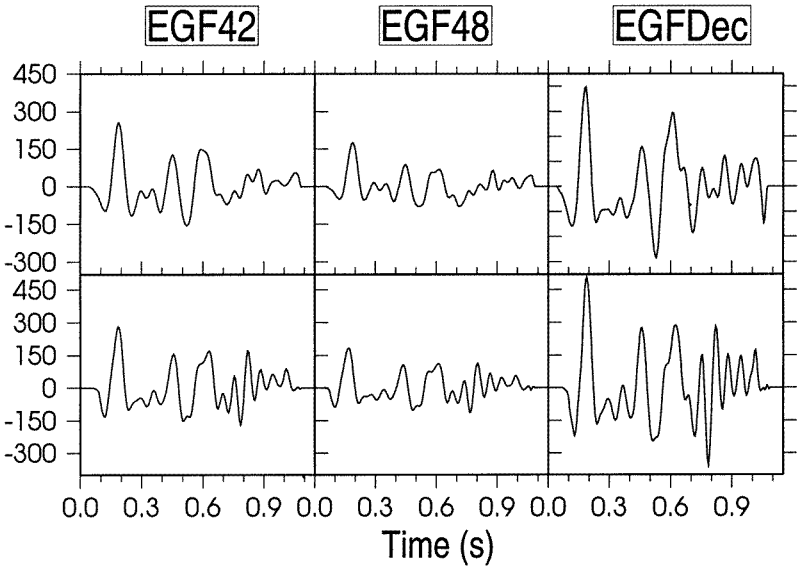


**Figure 10.** Comparison of the EGF used as initial guess (top panels) with those obtained by means of blind deconvolution (bottom panels). Case of MAIN5139, station IMI.

## 5. Concluding remarks

The blind-deconvolution method we propose has been presented in the case of the EGF model for the description of the seismic events. However, it is obvious that it can be applied to any deconvolution problem in one or more variables. The EGF must be replaced by the impulse response function of the linear system and the STF by its input. Moreover, the various constraints on these functions must be specified. If these are expressible in terms of convex sets, the projected Landweber method can be used for constrained deconvolutions and therefore our method can be put into practice. Other applications are in progress, in particular to the improvement of data in chirp-radar tomography [9]. The main feature of the method seems to be the fast convergence, so that only a few blind cycles are sufficient for obtaining reliable results.

In view of the specific application to seismology that we are considering in this paper, the following remarks seem to be relevant.

- The blind-deconvolution method is capable of furnishing a correct estimate of the STF even in critical cases, when the adopted EGF is not accurate.
- This result broadens the field of application of the method. For instance, as only noisy seismograms of small events (relatively far from the main shock) are recorded by our regional seismic networks, the choice of the most correct candidate as EGF could be very critical. The blind-deconvolution technique guarantees stable results independently of this choice.
- The corrected EGF, which represents a better estimate of the propagation term for the main shock, can be successfully used for further analyses. For example, the relative location procedure presented in [7] was necessarily limited to small events, but it could be extended to the largest events of the swarm by using the corresponding corrected EGF.

## References

[1] Bertero M, Bindi D, Boccacci P, Cattaneo M, Eva C and Lanza V 1997 Application of the projected Landweber method to the estimation of the source time function in seismology *Inverse Problems* **13** 465–86
[2] Bertero M and Boccacci P 1998 *Introduction to Inverse Problems in Imaging* (Bristol: IOP)
[3] Stockham T G, Cannon T M and Ingebretsen R B 1975 Blind deconvolution through digital signal processing *Proc. IEEE* pp 678–92
[4] Ayres G R and Dainty J C 1988 Iterative blind deconvolution method and its applications *Opt. Lett.* **13** 547–9
[5] Fish D A, Brinicombe A M and Pike E R 1995 Blind deconvolution by means of the Richardson–Lucy algorithm *J. Opt. Soc. Am.* A **12** 58–65
[6] Lagendijk R L and Biemond J 1991 *Iterative Identification and Restoration of Images* (Boston, MA: Kluwer)
[7] Cattaneo M, Augliera P, Spallarossa D and Eva C 1997 Reconstruction of seismogenetic structures by multiplet analysis: an example of Western Liguria, Italy *Bull. Seism. Soc. Am.* **87** 571–86
[8] Tikhonov A N, Goncharsky A V, Stepanov V V and Yagola A G 1995 *Numerical Methods for the Solution of Ill-posed Problems* (Dordrecht: Kluwer)
[9] Miyakawa M 1993 Tomographic measurements of temperature change in phantoms of the human body by chirp radar-type microwave computed tomography *Med. Biol. Eng. Comput.* **31** 331–6